ESTEEM Academic Journal
Vol. 19, Sept 2023, 145-157

Stability Analysis of Mass Transfer Effects on the Unsteady Stagnation-Point Flow Past a Permeable Sheet

Nur Syazana Rosly[1], Noraini Ahmad [2], Syakila Ahmad[3] and Norshafira Ramli [4]
[1, 2]*Centre of Foundation Studies, Universiti Teknologi MARA, Cawangan Selangor, Kampus Dengkil 43800 Dengkil, Selangor, Malaysia*
[3, 4]*School of Mathematical Sciences, Universiti Sains Malaysia, 11800 USM, Penang, Malaysia*
**corresponding author: [1]syazanarosly@uitm.edu.my*

ARTICLE HISTORY

Received
20 January 2023

Accepted
20 August 2023

Available online
30 September 2023

ABSTRACT

This study involves the problem of mass transfer effects on unsteady stagnation-point flow through a permeable stretching/shrinking sheet. Similarity transformations in the form of nonlinear partial differential equations to ordinary differential equations were used to reduce the basic governing equations. The resulting equations were then solved numerically using the `bvp4c` *function and shooting method. The programming codes for* `bvp4c` *function were built using Matlab software, whereas the programming codes for shooting method were built using Maple software. The effects of the Schmidt number, stretching/shrinking, suction/injection, unsteadiness and the reaction rate parameter on the flow and mass transfer characteristics were numerically analysed. The boundary layer thickness and velocity gradient are also influenced by these parameters. Dual solutions were figured out for the problems involving stretching/shrinking sheet at the stagnation-point. To determine the stability of the solutions obtained, stability analysis was performed by solving the linear eigenvalue problems using the bvp4c function. The analysis showed that for the first solution, there was an initial decay of disturbance, while the second and third solutions were opposite, where an initial growth of disturbance were detected for both. This result indicated that the first solution was more stable and physically realizable compared to others.*

Keywords: *boundary layer; unsteady; mass transfer; stagnation-point; stability analysis.*

1. INTRODUCTION

With the increasing amount of theoretical and experimental results on unsteady heat and mass transfer, the efforts in figuring out the problems related to unsteady mass transfer with chemical reactions seem to be quite demanding in order to gain more understanding on this matter. According to the study carried out by [1], it was found that one of the transformation which relates (for any given initial and boundary conditions) is the unsteady concentration field of a reactant of a first-order irreversible reaction to that of a solute (or equivalently, the unsteady temperature field). Based on this, the analysis will be generalized to consider the concentration fields of the reactants and the products of all types of first-order reactions in a steady flowing or stationary medium. A chemical reaction is a process involving one or more reactants, characterized by chemical changes, yielding one or more products which are different from the reactants. The reaction can be codified as either heterogeneous or homogeneous processes depending on whether they occur at an interface or as a single phase volume reaction. In well-

p-ISSN 1675-7939; e-ISSN 2289-4934

mixed systems, the reaction is heterogeneous if it takes place at an interface, and homogeneous, if it takes place in solution. In most cases of real chemical reactions, the reaction rate depends on the concentration of the species itself. Furthermore, a different order of chemical reaction greatly influences the mass transfer rate [2].

A reaction is said to be of first-order, if the rate of reaction is directly proportional to concentration. In many chemical engineering processes, there are chemical reactions between foreign mass and fluid. These processes may take place in many industrial applications such as food processing, manufacturing of ceramics and polymer production [3]. The steady flow and mass transfer with first-order chemical reaction in boundary layer stagnation point over a stretching/shrinking surface has been intensively studied by others, for example by [4-11]. Study done by [7] found that the concentration of boundary layer thickness decreases with the increasing values of Schmidt number and the reaction-rate parameter for both solutions. Other researchers [9] revealed that the dual solutions of velocity and concentration exist for certain values of velocity ratio parameter (the ratio of stretching/shrinking rate and straining rate). Recent works performed by [12] showed that the mass transfer of the first-order chemical reaction on a continuous flat plate moves with constant velocity in parallel or reversely to a uniform free stream. Our research is inspired by [7], by taking into account the influences of the suction/injection towards the unsteady stagnation-point flow.

As mentioned in the literature above, following mathematical model [7] will be applied for this problem. The reduced mathematical model can be obtained with the similarity transformations and worked out via the MATLAB program `bvp4c`. Interestingly, the presence of dual solutions (first and second solutions) will also be investigated. Consequently, the stability analysis will be done on dual solutions initiated by [13]. A key factor is how stability between the dual solutions is achieved. It offers a method to identify which solution is stable, as already done by other researchers [14-15] in their excellent paper on stability analysis.

2. MATHEMATICAL FORMULATION

Consider the two-dimensional unsteady stagnation-point flow of a laminar boundary-layer flow of an incompressible and viscous fluid over a stretching/shrinking sheet in the presence of a first-order chemical reaction as shown in Figure 1, where *x* and *y* are the Cartesian coordinate measured along and normal to the stretching/shrinking sheet. It is assumed that the velocity of the sheet is $u_x(x,t)$, while that of the ambient (inviscid) fluid is $u_e(x,t)$, where *t* is the time. It is also assumed that the constant species concentration at the surface of the sheet is C_w, while that of the ambient fluid is C_∞, where we assume that $C_w > C_\infty$. Further, it is assumed that the mass transfer velocity is $v_w(t)$, where $v_w(t) < 0$ corresponds to suction and $v_w(t) > 0$ corresponds to injection, respectively.

p-ISSN 1675-7939; e-ISSN 2289-4934

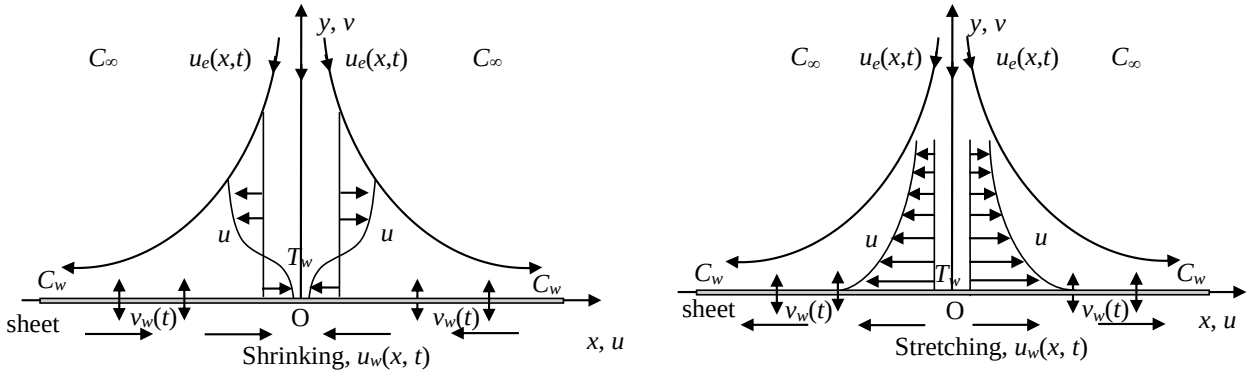

Figure 1: Physical model and coordinate system

Using Boussinesq approximation the governing equations for boundary layer flows and mass transfer can be written in Cartesian coordinate system as written in Equation 1, Equation 2 and Equation 3.

$$\frac{\partial u}{\partial x}+\frac{\partial v}{\partial y}=0, \tag{1}$$

$$\frac{\partial u}{\partial t}+u\frac{\partial u}{\partial x}+v\frac{\partial u}{\partial y}=\frac{\partial u_e}{\partial t}+u_e\frac{d\,u_e}{d\,x}+\nu\frac{\partial^2 u}{\partial y^2}, \tag{2}$$

$$\frac{\partial C}{\partial t}+u\frac{\partial C}{\partial x}+v\frac{\partial C}{\partial y}=D\frac{\partial^2 C}{\partial y^2}-\hat{r}(C-C_\infty). \tag{3}$$

Following [12] and [16] the appropriate boundary conditions are given by Equation 4.

$$\begin{aligned} &t<0: \quad v=0, \quad u=0, \quad C=C_\infty, \quad \text{for all } x, y, \\ &t\geq 0: \quad v=v_w(t), \quad u=u_w(x,t)=\frac{c\,x}{1-\gamma t}, \quad C=C_w(t)=C_\infty+\frac{C_0}{1-\gamma t} \text{ at } y=0, \\ &\qquad u\to u_e(x,t)=\frac{a\,x}{1-\gamma t}, \quad C\to C_\infty \quad \text{as} \quad y\to\infty. \end{aligned} \tag{4}$$

Here u and v are the components of velocity in the x and y directions, respectively, C is the species concentration in the fluid, where the concentration of the surface of the sheet is similarly assumed to vary both along the sheet and with time, in accordance with $C_w(t)=C_\infty+C_0/(1-\gamma t)$, where C_∞ is the constant free stream concentration. The wall concentration $C_w(t)$ represents a situation in which the sheet concentration increases (decreases) if C_0 is positive (negative), and such that the amount of concentration increases

p-ISSN 1675-7939; e-ISSN 2289-4934

(decreases) along the sheet with time. D is the molecular diffusivity of chemically reactive species, ν is the kinematic viscosity, and $\hat{r}$ is the rate of chemical conversion of the first-order homogeneous and irreversible reaction. We assume that $\hat{r} = r_0/(1-\gamma t)$ is the time-dependent reaction rate, where the variable reaction rate of the solute with r_0 being a constant initial reaction rate of chemical conversion, following [17] and γ being a constant with $\gamma t < 1$; the dimension of γ is (time)$^{-1}$. The diffusing species either can be destroyed or generated in the homogeneous reaction. Here, v_w is a prescribed variable distribution of suction or injection through the sheet and is given by Equation 5.

$$v_w(t) = -\sqrt{\frac{a\nu}{1-\gamma t}}\, s, \tag{5}$$

where s is the strength of the applied suction $(s > 0)$ or injection $(s < 0)$ parameter. These particular forms of $u_w(x,t)$, $C_w(t)$ and $v_w(t)$, which are valid for $t < \gamma^{-1}$, have been chosen in order to obtain a new similarity transformation that transforms the governing partial differential equations into a set of ordinary differential equations.

Referring to [18] similarity solutions exist only for flows which show certain inherent symmetry properties in space and time. A little inspection provides us a set of similarity solutions of the system of Equation 1, Equation 2 and Equation 3 which is similar to [12] and [17] (Equation 6):

$$\begin{aligned} u &= \frac{a\,x}{1-\gamma t} f'(\eta), \quad v = -\sqrt{\frac{\nu\, a}{1-\gamma t}}\, f(\eta), \\ \phi(\eta) &= \frac{C - C_\infty}{C_w - C_\infty}, \quad \eta = \sqrt{\frac{a}{\nu(1-\gamma t)}}\, y. \end{aligned} \tag{6}$$

The expressions of u and v identically satisfy the continuity Equation 1. By substituting values of u, v and C into equations (2) and (3), we get the following ordinary differential equations (Equation 7 and Equation 8):

$$f''' + f\, f'' + 1 - f'^2 - A\left(f' - 1 + \frac{\eta}{2} f''\right) = 0, \tag{7}$$

$$\frac{1}{\mathrm{Sc}}\phi'' - A\left(\phi + \frac{\eta}{2}\phi'\right) + f\phi' - R\phi = 0, \tag{8}$$

and the boundary conditions (4) reduce to the following forms (Equation 9):

p-ISSN 1675-7939; e-ISSN 2289-4934

$$\begin{aligned} &f(0)=s, \quad f'(0)=\lambda, \quad \phi(0)=1, \quad \text{at} \quad \eta=0, \\ &f'(\eta)\to 1, \quad \phi(\eta)\to 0 \quad \text{as} \quad \eta\to\infty, \end{aligned} \tag{9}$$

where $\mathrm{Sc}=\nu/D$ is the Schmidt number, $\lambda=c/a$ is the constant stretching $(\lambda>0)$ or shrinking $(\lambda<0)$ parameter, $A=\gamma/a$ is the unsteadiness parameter with $A>0$ for accelerating flow and $A<0$ for decelerating flow, respectively, and $R=r_0/a$ is the reaction rate parameter, where $R>0$ indicates destructive chemical reaction, $R<0$ denotes generative chemical reaction and $R=0$ represents the non-reactive species.

We notice that for a steady-state flow, $A=0$, Equation 2 and Equation 3 are reduced to the same as in [12] (Equation 10 and Equation 11):

$$f'''+f\,f''+1-f'^2=0, \tag{10}$$

$$\frac{1}{\mathrm{Sc}}\phi''+f\,\phi'-R\phi=0, \tag{11}$$

subject to the boundary conditions (Equation 9). Motivated by [12], we extended this problem to unsteady flow which includes an imposed time scale, in which the fluid velocity, pressure or density at a point changes with respect to time.

The quantities of physical interest are the skin friction coefficient C_f and the local Sherwood number Sh_x, which varies as shown as in Equation 12.

$$\mathrm{Re}_x^{1/2}C_f=f''(0), \qquad \mathrm{Re}_x^{-1/2}\mathrm{Sh}_x=-\phi'(0), \tag{12}$$

where $\mathrm{Re}_x=u_e(x)x/\nu$ is the local Reynolds number.

3. STABILITY ANALYSIS

Previous studies from [19-20] have demonstrated that the lower branch solutions are unstable (not realizable physically), while the upper branch solutions are more stable (physically realizable) for both forced convection boundary layer flow through a permeable flat plate, and mixed convection flow past a vertical flat plate. These characteristics are assessed by looking at the unsteady Equation 1 and Equation 2. Following [19], a new dimensionless time variable $\tau=at$ must be introduced. The use of τ is associated with an initial value problem and is consistent with the question of which solution will be obtained in practice. Using the variables τ and (6), the new dimensionless variables can be represented as in Equation 13.

p-ISSN 1675-7939; e-ISSN 2289-4934

$$u = \frac{a\,x}{1-\gamma\,t}\frac{\partial\, f}{\partial\,\eta}(\eta,\tau), \quad v = -\sqrt{\frac{\nu\,a}{1-\gamma\,t}}\,f(\eta,\tau),$$
$$\phi(\eta,\tau) = \frac{C-C_\infty}{C_w-C_\infty}, \quad \eta = y\sqrt{\frac{a}{\nu\,(1-\gamma\,t)}}, \tag{13}$$

so that Equation 2 and Equation 3 can be written as (Equation 14 and Equation 15)

$$\frac{\partial^3 f}{\partial\,\eta^3} + f\,\frac{\partial^2 f}{\partial\,\eta^2} + 1 - \left(\frac{\partial\, f}{\partial\,\eta}\right)^2 - A\left(\frac{\partial\, f}{\partial\,\eta} - 1 + \frac{\eta}{2}\frac{\partial^2 f}{\partial\,\eta^2}\right) - (1-A\,\tau)\frac{\partial^2 f}{\partial\,\eta\,\partial\,\tau} = 0, \tag{14}$$

$$\frac{1}{\mathrm{Sc}}\frac{\partial\phi^2}{\partial^2\eta} - A\left(\frac{\eta}{2}\frac{\partial\phi}{\partial\eta} - \phi\right) + f\,\frac{\partial\phi}{\partial\eta} - R\,\phi - (1-A\tau)\frac{\partial\phi}{\partial\tau} = 0, \tag{15}$$

subject to the boundary conditions (Equation 16)

$$f(0,\tau) = s, \quad \frac{\partial\, f}{\partial\,\eta}(0,\tau) = \lambda, \quad \phi(0,\tau) = 1,$$
$$\frac{\partial\, f}{\partial\,\eta}(\eta,\tau) \to 1, \quad \phi(\eta,\tau) \to 0 \quad \text{as} \quad \eta \to \infty. \tag{16}$$

The stability of the solution $f = f_0(\eta)$ and $\phi = \phi_0(\eta)$ that satisfy the boundary value problem Equation 7, Equation 8 and Equation 9is tested by introducing [19-21] (Equation 17)

$$f(\eta,\tau) = f_0(\eta) + e^{-\varepsilon\tau}\,F(\eta,\tau), \quad \phi(\eta,\tau) = \phi_0(\eta) + e^{-\varepsilon\tau}\,G(\eta,\tau), \tag{17}$$

where ε is an unknown eigenvalue parameter, and $F(\eta,\tau)$ and $G(\eta,\tau)$ are small corresponding to $f_0(\eta)$ and $\phi_0(\eta)$, respectively. By substituting Equation 17 into Equation 14 and Equation 15, the following linearized problem is obtained (Equation 18 and Equation 19):

$$\frac{\partial^3 F}{\partial\,\eta^3} + \left(f_0 - A\frac{\eta}{2}\right)\frac{\partial^2 F}{\partial\,\eta^2} + \left[\varepsilon\,(1-A\,\tau) - 2\,f_0' - A\right]\frac{\partial\, F}{\partial\,\eta} + f_0''\,F$$
$$-(1-A\,\tau)\frac{\partial^2 f}{\partial\,\eta\,\partial\,\tau} = 0, \tag{18}$$

p-ISSN 1675-7939; e-ISSN 2289-4934

$$\frac{1}{\mathrm{Sc}}\frac{\partial^2 G}{\partial \eta^2}+\left(f_0-A\frac{\eta}{2}\right)\frac{\partial G}{\partial \eta}+\left(A-R+(1-A\tau)\varepsilon\right)G+\phi_0' F - (1-A\tau)\frac{\partial G}{\partial \tau}=0, \tag{19}$$

subject to the boundary conditions (Equation 20)

$$F(0,\tau)=0,\quad \frac{\partial F}{\partial \eta}(0,\tau)=0,\quad G(0,\tau)=0,$$
$$\frac{\partial F}{\partial \eta}(\eta,\tau)\to 0,\quad G(\eta,\tau)\to 0 \quad \text{as} \quad \eta\to\infty. \tag{20}$$

To examine the stability of the steady flow $f_0(\eta)$ and $\phi_0(\eta)$ of Equation 18 and Equation 19, we need to set $\tau=0$, for which $F(\eta)=F_0(\eta)$ and $G(\eta)=G_0(\eta)$ are obtained to recognize which solution is the initial growth and which is the decay of the solution (Equation 17). Hence, the linearized problem (Equation 14) and (Equation 15) can be written as (Equation 21 and Equation 22

$$F_0''' +\left(f_0-A\frac{\eta}{2}\right)F_0'' +(\varepsilon-2f_0'-A)F_0' + f_0'' F_0=0, \tag{21}$$

$$\frac{1}{\mathrm{Sc}}G_0'' +\left(f_0-A\frac{\eta}{2}\right)G_0' +\left(A-R+\varepsilon\right)G_0+F_0\phi_0' =0, \tag{22}$$

along with the boundary conditions (Equation 23)

$$F_0(0)=0,\quad F_0'(0)=0,\quad G_0(0)=0,$$
$$F_0'(\eta)\to 0,\quad G_0(\eta)\to 0 \quad \text{as} \quad \eta\to\infty. \tag{23}$$

The possible range of the smallest eigenvalues can be found by following [22]. A boundary condition, either $F_0'(\eta)$ or $G_0(\eta)$ should be selected. For this problem, we choose the condition of $F_0'(\eta)\to 0$ as $\eta\to\infty$, and for a fixed value of ε we solve the system (Equation 21) and (Equation 22) along with the new boundary condition $F_0''(0)=1$[23].

4. RESULTS AND DISCUSSION

The system of ordinary differential Equation 7 and Equation 8subject to the boundary conditions (Equation 9) were solved numerically using shooting method. By considering two different values of boundary layer thickness for certain value of pertinent parameters, there might be two different velocity and concentration profiles as well as two different values of $f''(0)$ and $\phi'(0)$. Thus, both velocity and concentration profiles obtained should satisfy the given boundary conditions (Equation 9).

p-ISSN 1675-7939; e-ISSN 2289-4934

In order to assess the accuracy of our method, we compared our skin frictions coefficient, $\mathrm{Re}_x^{1/2} C_f$ for a steady-state flow ($A = 0$) with those of [9] and [24] where they used the `bvp4c` form Matlab and the Keller-box method, respectively. The results were found to be in an excellent agreement as shown in Table 1. Hence, they were regarded as correct and accurate.

Table 1: Comparison of the values of skin friction coefficient for several values of λ

λ	Present study		[9]		[24]	
	First Solution	Second Solution	First Solution	Second Solution	First Solution	Second Solution
–0.25	1.4022408		1.4022407		1.402241	
–0.50	1.4956698		1.4956697		1.495670	
–0.75	1.4892983		1.4892981		1.489298	
–1.00	1.3288170	0	1.3288168	0	1.328817	
–1.15	1.0822314	0.1167022	1.0822311	0.1167020	1.082233	0.116702
–1.20	0.9324738	0.2336497	0.9324733	0.2336496		
–1.2465	0.5842950	0.5542845	0.5842816	0.5542962	0.584303	0.554295
–1.24657	0.5745633	0.5639788	0.5745372	0.5640096		

Figure 2 portray the variation of skin friction coefficient $\mathrm{Re}_x^{1/2} C_f$ and the local Sherwood number $\mathrm{Re}_x^{-1/2} \mathrm{Sh}_x$, respectively, with λ for several values of unsteadiness parameter *A*. These figures show that $\mathrm{Re}_x^{1/2} C_f$ and $\mathrm{Re}_x^{-1/2} \mathrm{Sh}_x$ increase with the decrement of unsteadiness parameter. Dual solutions exist for both the shrinking and stretching sheet and the critical points are shown in Table 2. The effect of the suction parameter *s* against the skin friction coefficient $\mathrm{Re}_x^{1/2} C_f$ and $\mathrm{Re}_x^{-1/2} \mathrm{Sh}_x$ is plotted against λ in Figure 3 for an unsteady flow with $A = -1$ and for the first solution branch, $\mathrm{Re}_x^{1/2} C_f$ changes sign at $\lambda = 1$. This figure clearly shows that the effect of having fluid withdrawal through the surface is to decrease the critical value λ_c, again giving a greater range of negative λ for solutions in the shrinking sheet case, as can be seen in Table 2. The increment values of *s* will decrease the critical value λ_c, due to the fact that the momentum as well as the concentration boundary layer thickness decrease with suction.

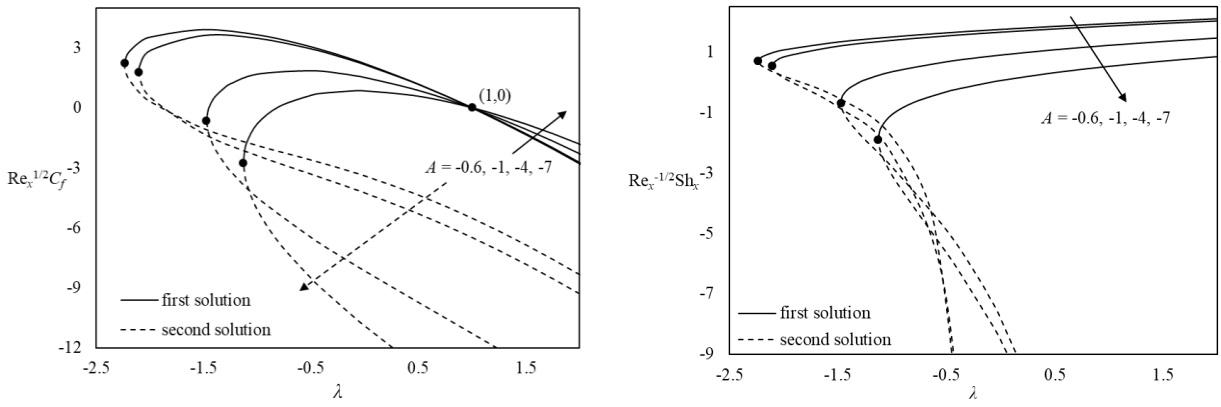

Figure 2: Variation of $\mathrm{Re}_x^{1/2} C_f$ and $\mathrm{Re}_x^{-1/2} \mathrm{Sh}_x$ over λ for several values of A when $s = 1.6$, $R = 0.1$ and $\mathrm{Sc} = 1$.

p-ISSN 1675-7939; e-ISSN 2289-4934

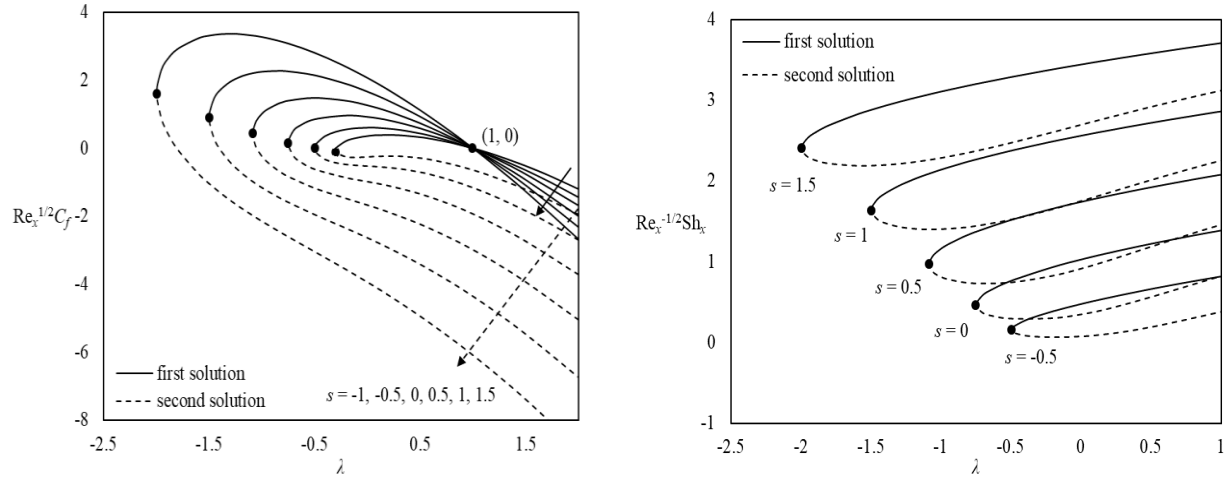

Figure 3: Variation of $\mathrm{Re}_x^{1/2} C_f$ and $\mathrm{Re}_x^{-1/2} \mathrm{Sh}_x$ over λ for several values of using $R = 1$, $A = -1$ and $\mathrm{Sc} = 2$.

Table 2: Value of the critical points λ_c for different paramater

Figures	s	A	λ_c
2	1.6	–0.6	–2.23525
		–1	–2.10556
		–3	–1.47224
		–7	–1.12838
3	–1	–1	–0.30560
	–0.5		–0.49547
	0		–0.75177
	0.5		–1.08222
	1		–1.49413
	1.5		–1.99438

Figure 4 shows the skin friction coefficients $\mathrm{Re}_x^{1/2} C_f$ for various values of shrinking $\lambda < 0$ parameter, versus parameter suction/injection parameter *s*. The $\mathrm{Re}_x^{1/2} C_f$ increases as the shrinking parameter λ decreases for both the first and second solutions. As $\lambda \to -\infty$, solutions only exist for the mass suctions parameter $s > 0$. However, as $\lambda \to 0$, the solutions extend more to the left, and this gives dual solutions for both suction/injection parameter *s*. Figure 4 also shows $\mathrm{Re}_x^{-1/2} \mathrm{Sh}_x$ for various values of shrinking parameter $\lambda < 0$ versus *s* when $R = 0.5$, $\mathrm{Sc} = 1$ and $A = -1$. As the magnitude of λ increases, it will give an increment for the mass transfer rate. Same as $\mathrm{Re}_x^{1/2} C_f$, as $\lambda \to -\infty$, solutions only exist for the mass suctions parameter $s > 0$. However, as $\lambda \to 0$ the solutions extend more to the left, and this gives dual solutions for both the suction and injectio parameter *s*.

The variations $\mathrm{Re}_x^{-1/2} \mathrm{Sh}_x$ for $R > 0$ indicates destructive chemical reaction, $R < 0$ denotes generative chemical reaction and $R = 0$ represents the non-reactive species are presented in Figures 5(a) and Figure 5(b) for $\mathrm{Sc} = 0.5$ and $\mathrm{Sc} = 1$ respectively. Both figures presented three values of R i.e., $R = -0.5$, 0, 0.5 and for the first solutions branch, the mass transfer rate increases as the reaction rate parameter increases. When $R > 0$, the destructive chemical

p-ISSN 1675-7939; e-ISSN 2289-4934

reactions will take place and at the end of the reaction, some molecules will disappear. The boundary layer thickness of the chemical species concentration will decrease when R ranges from negative to positive. Since the concentration gradient increases, the rate of mass transfer will also increase. However, the flow separation occurs for the second solutions when $R<0$ for $\mathrm{Sc}=0.5$ and when $R\le 0$ for $\mathrm{Sc}=1$. Note that the variation of R and Sc only affects $\mathrm{Re}_x^{-1/2}\,\mathrm{Sh}_x$.

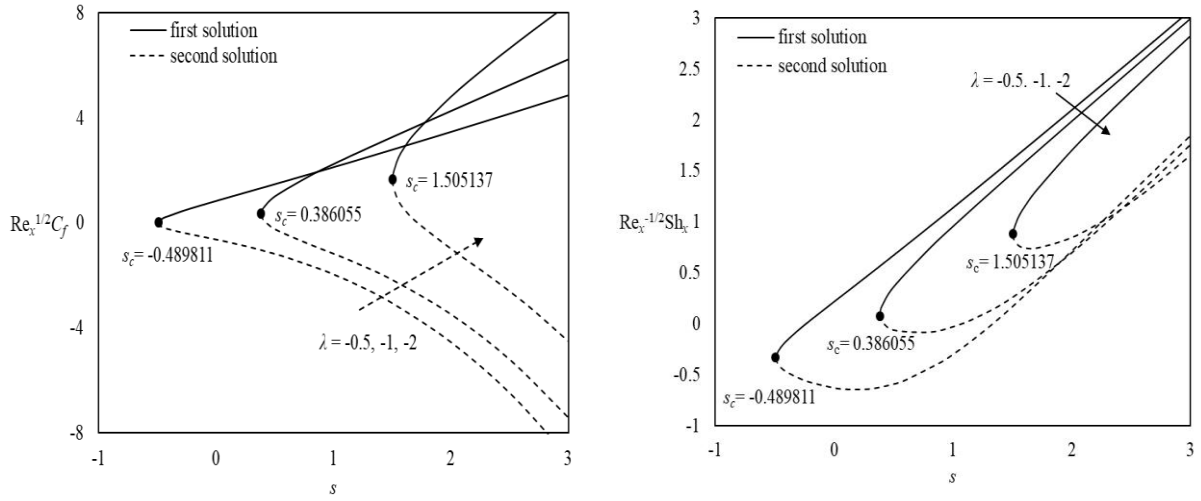

Figure 4: Variation of $\mathrm{Re}_x^{1/2}\,C_f$ and $\mathrm{Re}_x^{-1/2}\,\mathrm{Sh}_x$ over s for several values of λ when $\mathrm{Sc}=1$, $R=0.5$ and $A=-1$

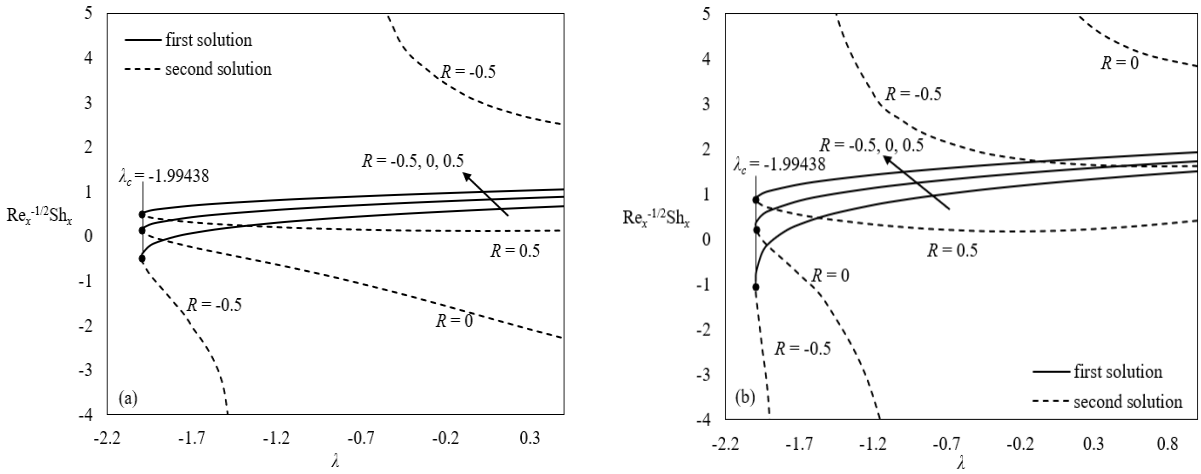

Figure 5: Variation of $\mathrm{Re}_x^{-1/2}\,\mathrm{Sh}_x$ over λ for several values of R when when (a) $\mathrm{Sc}=0.5$, (b) $\mathrm{Sc}=1$, $s=1.5$ and $A=-1$

The velocity $f'(\eta)$ and concentrations $\phi(\eta)$ profiles for several values of s in the case of shrinking sheet ($\lambda=-1$) when $A=-1$, $R=0.1$ and $\mathrm{Sc}=1$ are depicted in Figure 6 (a) and

p-ISSN 1675-7939; e-ISSN 2289-4934

Figure 6(b), respectively. With the increasing of s , fluid velocity is found to increase, as seen in Figure 6(a). Suction causes the increment of the velocity of fluid inside the boundary layer. By sucking fluid particles through permeable plate, the momentum of boundary layer thickness is reduced. Consequently, the velocity will increase. However, when fluid particles are injected, ($s < 0$) the momentum of boundary layer thickness becomes larger. Figure 6(b) shows that the dimensionless concentration $\phi(\eta)$ decreases with the increasing suction parameter, and the solute boundary layer thickness decreases with the suction parameter ($s > 0$) . Due to this, the rate of mass transfer will also increase. On the other hand, the concentration increases with the increase of injection or blowing parameter ($s < 0$).

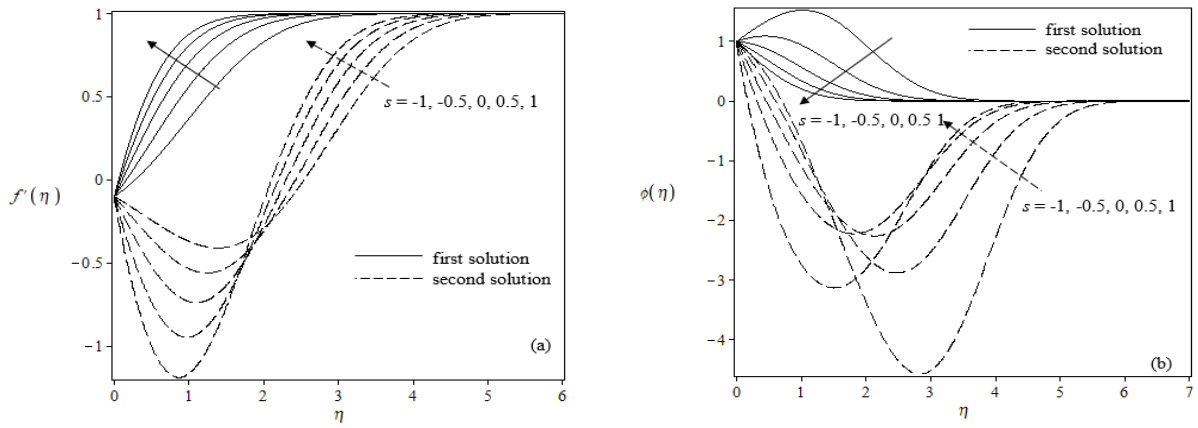

Figure 6: (a) Velocity, (b) concentration profiles for several values of s in the case of shrinking sheet ($\lambda = -1$) when $A = -1$, $R = 0.1$ and $\mathrm{Sc} = 1$

Table 3: Smallest eigenvalues of ε for several values of A and λ when $s = 1.6$, $R = 0.1$ and $\mathrm{Sc} = 1$

A	λ	ε First solution	ε Second solution
–0.6	–2.23	0.23863	–0.23368
λ_c = –2.23525	–2.2	0.61465	–0.58262
	–2.15	0.96377	–0.88649
	–2.1	1.22107	–1.09837
–1	–2.05	0.79564	–0.74668
λ_c = –2.10556	–2.0	1.10560	–1.01251
	–1.9	1.55784	–1.37638
	–1.8	1.91071	–1.64080
–4	–1.47	0.19061	–0.18883
λ_c = –1.472235	–1.45	0.60647	–0.58873
	–1.4	1.10382	–1.04628
	–1.3	1.72224	–1.34725
–7	–1.12	0.43181	–0.42523
λ_c = –1.12838	–1.105	0.72135	–0.70316
	–1.1	0.7953	–0.77325
	–1.0	1.71055	–1.61144

p-ISSN 1675-7939; e-ISSN 2289-4934

Dual solutions were also obtained in this problem. A stability analysis was conducted by solving unidentified eigenvalue ε in Equation 21 and Equation 22, alongside with the boundary conditions (Equation 23) using `bvp4c` function. The smallest eigenvalues ε for different values of A and λ are shown in Table 3 where the results clearly show that positive eigenvalues ε, were obtained for the first solution, while second solution showed the contrast. Therefore, it can be concluded that the first solution is stable and physically realizable while the second solution is unstable and not physically realizable.

5. CONCLUSION

This study reveals that dual solutions seem to exist for both shrinking sheet ($\lambda < 0$) and stretching sheet ($\lambda > 0$) in decelerating flow ($A < 0$). It was found that the fluid velocity was initiallylow due to the increment of unsteadiness parameter. Other than that, concentration was also significantly lower. For the given Schmidt number, it was observed that the concentration increases during a generative chemical reaction and decreases in a destructive chemical reaction. The generative first-order chemical reaction effect ($R < 0$) produces thicker concentration of boundary layers, while the destructive first-order chemical reaction effect ($R > 0$) has the tendency to reduce the thickness of boundary layer. Due to increment of suction at the plate, the momentum and concentration of boundary layer thicknesses reduce, while for injection/blowing, both boundary layers become thicker. The reactive concentration profile at a fixed point decreases with increasing Schmidt number and reaction rate parameter. For small Schmidt number, mass absorption may occur in some cases of constructive chemical reaction. The stability analysis shows that the first solution is stable while the second was unstable.

CONFLICT OF INTEREST

The authors declare no conflict of interest.

REFERENCES

[1] P. V. Danckwert, "Absorption by simultaneous diffusion and chemical reaction into particles of various shapes and into falling drops," *Transactions of the Faraday Society*, vol 47, pp. 1014–1023, 1951.

[2] S. Zainodin, A. Jamaludin, R. Nazar and I. Pop, "Effects of higher order chemical reaction and slip conditions on mixed convection hybrid ferrofluid flow in a Darcy porous medium," *Alexandria Engineering Journal*, vol. 68, no. 1, pp. 111–126, 2023.

[3] R. Muthucumaraswamy, and S. Meenakshisundaram, "Theoretical study of chemicalreaction effects on vertical oscillating plate with variable temperature and mass diffusion," *Journal of Theoretical and Applied Mechanics*, vol. 3, no. 3, pp. 245–257, 2006.

[4] H. I. Andersson, O .R. Hansen and B. Olmedal, "Diffusion of a chemically reactive species from a stretching sheet," *International Journal Heat Mass Transfer*, vol. 37, pp. 659–664, 1994.

[5] H. S. Takhar, A. J. Chamkha and G. Nath, "Flow and mass transfer on a stretching sheet with a magnetic field and chemically reactive species," *International Journal of Engineering Sciences*, vol. 38, pp. 1303–1314, 2000.

[6] R. Cortell, "MHD flow and mass transfer of an electrically conducting fluid of second grade in a porous medium over a stretching sheet with chemically reactive species," *Chemical Engineering and Processing*, vol. 46, pp. 721–728, 2007.

[7] K. Bhattacharyya, "Dual solutions in boundary layer stagnation-point flow and mass transfer with chemical reaction past a stretching/shrinking sheet," *International Communication in Heat Mass Transfer*, vol. 38, pp. 917–922, 2011.

p-ISSN 1675-7939; e-ISSN 2289-4934

[8] K. Bhattacharyya, "Boundary layer flow with diffusion and first-order chemical reaction over a porous flat plate subject to suction/injection and with variable wall concentration," *Chemical Engineering Research Bulletin*, vol. 15, pp. 6–11, 2011.

[9] N. C. Roşca, T. Grosan, and I. Pop, "Stagnation-point flow and mass transfer with chemical reaction past a permeable stretching/shrinking sheet in a nanofluid," *Sains Malaysiana*, vol. 40, no. 10, pp. 1271–1279, 2012.

[10] N. Najib, N. Bachok, N. Arifin and A. Ishak, "Stagnation Point Flow and Mass Transfer with Chemical Reaction past a Stretching/Shrinking Cylinder," *Sci Rep*, vol. 4, 4178, 2014.

[11] S. H. Reddy, K. N. Kumaraswamy, D. H. Babu and P. V. S. Narayanal, "Significance of chemical reaction on MHD near stagnation point flow towards a stretching sheet with radiation," *SN Applied Sciences*, vol. 2, p. 1822, 2020.

[12] K. Bhattacharyya, " Dual solutions in boundary layer stagnation-point flow and mass transfer with chemical reaction past a stretching/shrinking sheet," *International Journal of Heat and Mass Transfer*, vol. 55, pp. 3482–3487, 2012.

[13] P. Weidman and M. R. Turner, "Stagnation-point flows with stretching surfaces: A unified formulation and new results," *European Journal of Mechanics-B/Fluids*, vol. 61, pp. 144–153, 2017.

[14] N. S. Anuar, N. Bachok, N. M. Arifin and H. Rosali, "Effect of suction/injection on stagnation point flow of hybrid nanofluid over an exponentially shrinking sheet with stability analysis," *CFD Letters*, vol. 11, no. 12, pp. 21-33, 2019.

[15] I. Waini, A. Ishak and I. Pop, "Hybrid nanofluid flow towards a stagnation point on an exponentially stretching/shrinking vertical sheet with buoyancy effects," *Int. J. Numer. Meth. Heat Fluid Flow*, vol. 31, no. 1, pp. 216-235, 2020.

[16] S. Mukhopadhyay and K. Bhattacharyya, " Unsteady flow of a Maxwell fluid over a stretching surface in presence of chemical reaction," *Journal of the Egyptian Mathematical Society*, vol. 20, pp. 229–234, 2012.

[17] M. A. El-Aziz, "Unsteady fluid and heat flow induced by a stretching sheet with mass transfer and chemical reaction," *Chemical Engineering Communications*, vol. 197, no. 10, pp. 1261–1272, 2010.

[18] C. Y. Wang, "Exact solutions of the unsteady Navier-Stokes equations," *Applied Mechanics Reviews*, vol. 42, no. 11S, pp. S269–S282, 1989.

[19] P. D. Weidman, D. G Kubittschek and A. M. J. Davis, "The effect of transpiration on self-similar boundary layer flow over moving surfaces," *International Journal Engineering Sciences*, vol. 44, pp. 730–737, 2006.

[20] A. V. Roşca and I. Pop, "Flow and heat transfer over a vertical permeable stretching/shrinking sheet with a second order slip," *International Journal of Heat Mass Transfer*, vol. 60, pp. 355–364, 2013.

[21] N. Najib, N. Bachok and N. M. Arifin, "Stability of dual solutions of mass transfer on a continuous flat plate moving in parallel or reversely to a free stream in the presence of a chemical reaction with second order slip," *AIP Conference Proceedings*, vol. 1830, pp. 020009, 2017.

[22] S. D, Harris, D. B Ingham and I. Pop, "Mixed convection boundary–layer flow near the stagnation point on a vertical surface in a porous medium: Brinkman model with slip," *Transport Porous Media*, vol. 77, pp. 267–285, 2009.

[23] N. F. Dzulkifli, N. Bachok, N. A. Yacob, N. M. Arifin and H. Rosali, "Unsteady Stagnation-Point Flow and Heat TransferOver a Permeable Exponential Stretching/ShrinkingSheet in Nanofluid with Slip Velocity Effect: A Stability Analysis," *Applied Sciences*, vol. 8, p. 2172, 2018.

[24] Y. Y Lok, A. Ishak, and I. Pop, "MHD stagnation-point flow with suction towards a shrinking sheet," *Sains Malaysiana*, vol. 40, no. 10, pp. 1179–1186, 2011.

p-ISSN 1675-7939; e-ISSN 2289-4934